Journal of Renewable Materials

Tech Science Press

DOI: 10.32604/jrm.2021.015849

ARTICLE

Combined Recycling of White Rice Husk Ash as Cement Replacement and Metal Furnace Slag as Coarse-Aggregate Replacement to Produce Self-Consolidating Concrete

Naphol Yoobanpot[1,*], Prakasit Sokrai[2] and Natt Makul[2]

[1]Department of Civil Engineering, Faculty of Engineering, King Mongkut's University of Technology North Bangkok, Bangkok, 10800, Thailand

[2]Department of Civil Engineering Technology, Faculty of Industrial Technology, Phranakhon Rajabhat University, Bangkok, 10220, Thailand

[*]Corresponding Author: Naphol Yoobanpot. Email: naphol.y@eng.kmutnb.ac.th

Received: 18 January 2021 Accepted: 23 February 2021

ABSTRACT

According to empirical evidence, high levels of energy and considerable amounts of natural resources are used in the production of concrete. Given the context, this study explores self-consolidating concrete (SCC) that includes rice husk ash (RHA) and metal furnace slag (MFS) as an alternative to cement and the natural aggregates in standard SCC mixes. In this study, mixture designs are investigated with 20 wt.% of RHA, 10–30 wt.% of MFS and water-to-powder material ratios of 0.30 and 0.40. Based on the findings regarding the fresh-state, hardened-state, and durability properties of the resulting SCC mixes, it is evident that the use of RHA and MFS can significantly improve the properties of concrete. The highest compressive strength was achieved for SCC with 20 wt.% RHA and 10 wt.% MFS. This outcome should be used as a basis for further investigations into the production of concrete materials that are both high-performance and sustainable.

KEYWORDS

White rice husk ash; metal furnace slag; self-consolidating concrete; cement replacement; coarse-aggregate replacement

1 Introduction

Increased use of cement and concrete around the globe has recently become a subject of great importance in the construction industry, leading to a focus on identifying appropriate materials with which to replace the cement and the natural aggregates that are used in standard concrete mixtures. The relevant literature includes multiple studies that explore the relative viability of a range of materials as replacements or partial replacements for cement and/or its natural aggregates, such as rice husk ash (RHA) in place of cement and metal slag in place of concrete aggregate [1]. A review of these studies indicates that using steel slag in concrete construction with coarse aggregate achieved a compressive strength of 30 N/mm^2 and sufficient durability for low-grade use after 28 days of curing [2,3].

On the other hand, several alternatives have been proposed, including the use of steel slag as a replacement at approximately 40 wt.% for fine aggregates [4]. However, the durability of concrete that includes metal furnace slag (MFS) in its composition is a matter of concern, as this waste product tends

to reduce the strength of the concrete into which it is incorporated over time [5]. Yet, the fact remains: Steel slag has been used successfully to produce concrete that is characterized by adequate strength, sufficient durability, and extraordinary fracture properties in the short term [6].

As the construction industry continues to develop in an effort to meet increasing demand, high performance standards, and the goals pertaining to improving sustainability, self-consolidating concrete (SCC) has been considered as a possible replacement for the cement and the natural aggregates used in ordinary concrete. Since its development in Japan in the 1980s, SCC has become commonplace globally, with an increase in the number of applications for which it has been used [7]. Despite the use of substitutes for cement and natural aggregates in SCC, it is still similar to ordinary concrete inasmuch as a high percentage of SCC's composition consists of cement, coarse and fine aggregates, and other natural aggregates.

When compared with conventional concretes, which only have slump limits, the three main attributes of SCC are its greater ability to flow with less vibration and to flow through congested reinforcement, as well as its ability to achieve homogeneity without its aggregates becoming segregated [8]. As a result of these defining attributes, SCC has been found to improve the quality of the concrete structure [9]. Further, in comparison with ordinary concrete, SCC entails a significant reduction in coarse aggregates, while the fine aggregates that are required increase with respect to the rheological properties [10]. In addition, it has also been established that vibration is no longer required to compact SCC [10].

In an effort to improve the quality of the concrete structure, several attempts have been made to achieve desirable properties. For instance, the durability of SCC in combination with MFS was examined, with the results indicating that SCCs that include metal slag in their composition are both stronger and more durable than the control SCC [11]. Further, based on a study by Qasrawi [12], it was discovered that used to replace the coarse aggregate at 50 wt.% the new materials were responsible for the new properties.

According to several studies, SCC is associated with the qualities of SCC are most effective when pozzolanic materials such as RHA are included in its mix [13,14]. This result is in contrast to agro-industrial residues, which are more suitable than RHA for use as biomass. Due to its presence in large volumes around the globe, RHA is considered a suitable replacement for cement in concrete production [15].

Numerous studies have been conducted on how RHA can be used in the production of concrete, with each study focusing on a small number of properties, or even one property, rather than looking at the range of properties that need to be considered in producing concrete that is suitable for a given use [12,16]. RHA can not only be used in concrete but also carries the potential for use in geopolymer binders. The study shows that the optimum amount for replacement with RHA is 5%, which results in a 2.81% decrease in slump-flow value but increases by 3.02% the compressive strength in comparison to the control geopolymer. These test results were confirmed through microstructure investigation, with the SEM images of a 5% RHA mix demonstrating increased density [17].

In addition, RHA has the potential to be applied as a pozzolanic material, which was demonstrated by the later gain in compressive strength at 45 days [18]. Le and Ludwig examined the workability properties of SCC that includes RHA in its composition and discovered an improvement in tensile strength and viscosity as compared with these properties in SCC without RHA. The improvements were attributed to particle size as the RHA enhanced the viscosity and yield level of the SCC [19]. Furthermore, combining RHA with SCC tended to reduce the temperature of the concrete significantly while enhancing flowability, mass distribution, and mechanical performance during its use in construction [20].

2 Research Significance

Historically, concrete has consisted of a mixture of cement and natural aggregates. Most studies that have assessed the properties of concrete associate its production with high levels of gas emissions, given that its production requires a large amount of energy and natural resources compared to other

construction materials. Possible alternatives have been developed whereby an SCC is produced with the materials that are ordinarily used in concrete production being entirely or partially replaced with less expensive and/or more sustainable material or materials [21]. However, most of the studies fail to offer a concrete mix design procedure to use in the production of the proposed SCC mixture. In this study, SCC samples are investigated with a focus on rendering improvements to the properties of standard SCC (the control) in order to advance the production of more sustainable, less expensive SCC that can offer an acceptable or even higher level of performance.

The literature includes very few studies that focus on the main properties of SCC that include RHA and/or MFS as a possible replacement for cement and/or natural aggregates [22,23,24]. Given this gap in the research, in the present paper, through an experimental design, the properties of fresh state, hardened state, and the durability of SCC with both RHA and MFS included in its composition are explored via a comparison with those of standard concrete, which consists entirely of conventional materials.

3 Materials and Methods

An experimental design is adopted to explore the impact of replacing cement and natural aggregates in a standard SCC with RHA together with MFS in several proportions. The study focuses on three properties—the fresh state, the hardened state, and durability—as a basis for comparing these mixtures with a standard SCC (the control mixture).

A common feature associated with the SCC and the control SCC is a water-to-powder materials ratio (w/p) proportion ranging from 0.30 to 0.40, which is employed in the study. Based on the guidelines presented by the European Federation of National Associations Representing Producers and Applicators of Specialist Building Products for Concrete (EFNARC) [25], 0.97 L per 100 kg of powder materials of Type-G superplasticizer (42.5% solid content) in the SCC admixture was used to achieve a flow of 67.5 ± 2.50 cm. On this basis, the SCC would be able to flow through tight openings in reinforced metal without the need for either a separation or a blockage. MFS was included in the SCC mixes in various proportions, ranging from 0 to 30 wt.%.

3.1 Materials

Several materials were considered in evaluating the SCC mixtures that include RHA and MFS in their composition.

The first material was the SCC mixture, which was created using OPC with a gravity of 3.14, as defined by ASTM C150 [26]. The second material was RHA, which was obtained at a thermal power station in Thailand under controlled conditions, including a maximum burning temperature and an oxygen content in the burning chamber of 780°C and 55 vol.%, respectively, by using directly as-received RHA and no any treatment method. The third material considered was MFS, which was salvaged from the engine parts casting process using a basic oxygen furnace. It is essential to take several steps in order to obtain this by-product. First, the mold must be separated from the different types of irons in the iron-melting process. Second, the scrap metal must be cleaned by sandblasting in order to eliminate the iron and any dirt. Finally, the scrap must be transferred to a melting chamber in a melting furnace at a temperature of 1500°C. The MFS obtained in the present study was subjected to grinding in a Los Angeles grinding machine for 45 min at 550 rpm/min. A critical evaluation of these materials indicates that each is identified using diverse chemical compositions and physical properties of cement and admixtures (Tab. 1). The distribution of different particle sizes used in OPC and RHA is provided in Fig. 1(a), and the gradations of MFS and the conventional coarse aggregate used in compliance with ASTM C33 [27] are shown in Fig. 1(b). The average particle size of OPC, RHA, and MFS at 50 vol.% cumulative passing was observed as 10.22 μm, 22.57 μm, and 7.14 mm, respectively. Further, a morphology showing the micrograph at approximately 5000× magnification of the OPC, RHA, and MFS was used (Fig. 2). It was found that the OPC particles were smaller than those of the RHA and the MFS. The RHA particles had high porosity. Moreover, when comparing the surface characteristics of each

material, it was found that RHA was rough and coarse, more like a layered sheet, which had an effect on increasing its water absorbency, while OPC and MFS have surfaces that are smoother and more angular, with has smaller particles attached to it.

Table 1: Chemical composition and physical properties of OPC, RHA, and MFS

Material	Chemical composition (% by mass)								
	SiO_2	Al_2O_3	Fe_2O_3	MgO	CaO	Na_2O	K_2O	SO_3	LOI
OPC	21.33	5.29	3.17	1.11	68.34	0.29	0.18	0.96	0.71
RHA	93.22	0.47	0.34	0.46	1.09	0.45	1.49	0.73	1.26
MFS	55.74	12.66	17.05	0.41	1.67	0.04	0.53	0.02	0.90

Physical property	OPC	RHA	MFS
Particle size at 50% cumulative passing	10.22 μm	22.57 μm	7.14 mm
Specific gravity	3.14	2.36	5.72
Specific surface area (BET method) (m^2/kg)	1245	960	65
Density (kg/m^3)	1598.20	625.17	213.75
Pozzolanicity (Chapelle test) (mg CaO/g sample)	Not applicable	837.04	Not applicable

The fourth material considered in the experimental mix design was crushed limestone rock as a coarse aggregate, which is to be inert material and does not react with the alkali in cement over the long term. The coarse aggregate used had a nominal maximum size of 0.63 in. (1.60 cm), a gravity of 2.70, fineness of 7.18, and a density of 1555 kg/m^3. The fifth material considered was washed sand from a river with a fine aggregate of 0.475 cm, gravity of 2.62, fineness of 2.75, and density of 1688 kg/m^3. These aggregates were required to conform to the recommended curves, as outlined in ASTM C33 [26]. For the particle size distribution of MFS (Fig. 1) compared to that of the coarse aggregate (crushed limestone rock), the requirements for ASTM C33 [26] found that the MFS had a larger particle distribution than the marginal region. This is due to the limitations of the Los Angeles grinding method. However, the tendency of the mixed size distribution is similar to that of the coarse aggregate used as a comparable aggregate, allowing it to be blended and formed into SCC.

Lastly, a Type-G superplasticizer was utilized in the experiment to improve workability and place ability. The superplasticizer consisted of a mixture of poly-carboxylic, ether-based material with a solid concentration of 42.5%, as outlined in the ASTM C494 specifications [27].

3.2 Preparation of the SCC Specimens

Several steps were taken to achieve a high level of uniformity among the SCC specimen mixtures as described in the previous section. The mixing sequence of the SCC started with mixing the fine and coarse aggregates for approximately one minute. Next, the OPC, RHA, and MFS were added to the initial mixture consisting of the fine and coarse aggregates; the resulting mixture was mixed for approximately four minutes until a dry state was achieved. Lastly, water and super-plasticizer were blended in a flask at a slow rate of 35 rpm.

SCC has three characteristics that improve its workability properties, namely, filling capacity, passing ability, and resistance to segregation [25,27]. The produced SCC mixtures, shown in Tab. 2, were tested immediately in order to evaluate its slump flow, as defined by ASTM C1611 [27]. The passing ability of

the SCC was evaluated in relation to the difference between two properties, namely, the slump flow and the J-ring flow, which influences the duration of SCC in the V-funnel, as outlined by ASTM C1621 [27]. Additionally, a V-funnel was employed to evaluate filling capacity and to prevent the materials constituting the concrete specimen from becoming segregated. The fresh density (unit weight) was noted, as outlined in the ASTM C138 [27].

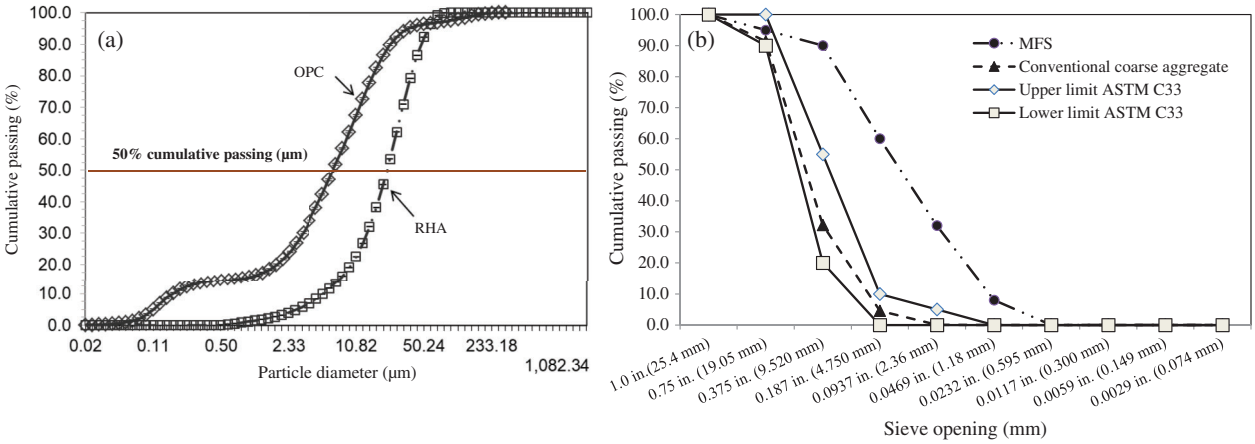

Figure 1: (a) Particle size distributions of OPC and RHA and (b) Gradations of MFS and conventional coarse aggregate used in compliance with ASTM C33 [26]

In regard to the hardened properties, it was important for the SCC mixtures to be cured in plastic sheets for 23½ h after mixing and demolding. Next, the SCC mixtures were subjected to the saturated-lime curing process within a controlled environment at 25°C until testing time. In this case, the sampled SCC mixtures were 15.2 cm in diameter × 30.4 cm in height, with their height being cast to measure the splitting tensile strength as outlined in ASTM C496 [27] at intervals of 3, 7, 28, 60, 90, 180, and 360 curing days. Additionally, the compressive strength of the SCC specimens was evaluated at similar intervals, as outlined in ASTM C39 [27]. A test to determine the modulus of elasticity was performed on the SCC specimens on the 360th curing day, as recommended by ASTM C469 [26].

The durability properties of the SCC specimens were evaluated using a sulfate solution attack and acetic acid (CH_3COOH) test. In the sodium sulfate (Na_2SO_4) test, the sampled SCC with an approximate size of 7.5 × 7.5 × 28.5 cm^3 was exposed to a 5.0% sodium sulfate solution for 360 curing days. During this period, the specimens were examined for changes in expansion at intervals of 7, 28, 90, 180, 270, and 360 days of curing, as outlined in ASTM C1012 [27]. The control SCC was also subjected to the same sodium sulfate solution to compare its results with those of the SCC specimens. Further, in the acid attack test, the SCC specimens with an approximate size of 10.0 × 10.0 × 10.0 cm^3 were exposed to a 3% concentration acetic (CH_3COOH) solution. After being immersed in the CH_3COOH solution at 7, 28, 90, 180, 270, and 360 days of curing, each sample concrete was washed and rinsed using distilled water and its weighted mass loss measured. The acid resistance capacity of each SCC specimen was assessed based on its ability to resist acid attack on its surface in terms of mass loss in the SCC specimen.

4 Results and Discussion

In this section, the properties of the SCC specimens with RHA and MFS are examined using the results obtained from the experiment and compared with those of the control SCC, i.e., the SCC that includes cement and natural aggregates in its composition. The properties of the SCC specimens and the control SCC are

examined in terms of their fresh-state, hardened-state, and durability properties. The results pertaining to each property are presented and discussed in the upcoming sections.

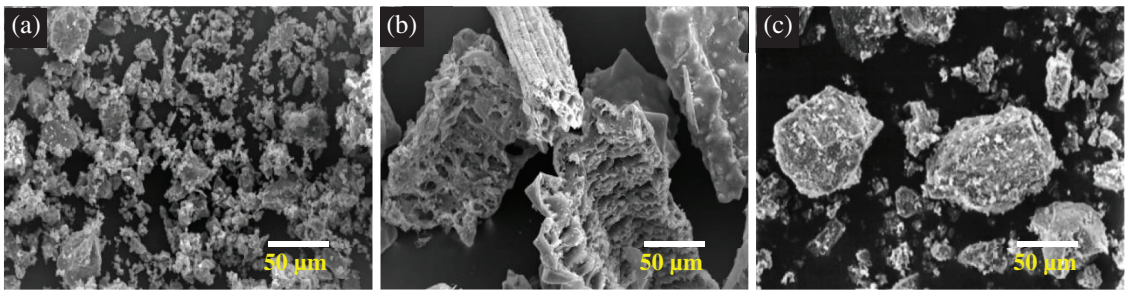

Figure 2: SEM micrographs (5000×) of (a) OPC, (b) RHA, and (c) MFS

Table 2: Mix design of SCC

Mixture label	w/p ratio	Powder materials (kg/m^3)	OPC (kg/m^3)	RHA lb/yd^3 (kg/m^3)	Sand lb/yd^3 (kg/m^3)	Crushed limestone rock lb/yd^3 (kg/m^3)	MFS lb/yd^3 (kg/m^3)	Water lb/yd^3 (kg/m^3)	High-range water-reducing admixture Type G [26]
55R0MFS0 [1]	0.30	550.0	550.0	0	931.0	811.0	0	165.0	5.34 L
55R20MFS0	0.30	550.0	440.0	110.0	931.0	811.0	0	165.0	5.34 L
55R20MFS10	0.30	550.0	440.0	110.0	931.0	730.0	81.0	165.0	5.34 L
55R20MFS30	0.30	550.0	440.0	110.0	931.0	568.0	243.0	165.0	5.34 L
55R0MFS0	0.40	550.0	550.0	0	852.0	742.0	0	220.0	5.34 L
55R20MFS0	0.40	550.0	440.0	110.0	852.0	742.0	0	220.0	5.34 L
55R20MFS10	0.40	550.0	440.0	110.0	852.0	668.0	74.0	220.0	5.34 L
55R20MFS30	0.40	550.0	440.0	110.0	852.0	520.0	222.0	220.0	5.34 L
65R0MFS0	0.30	650.0	650.0	0	842.0	734.0	0	195.0	6.31 L
65R20MFS0	0.30	650.0	520.0	130.0	842.0	734.0	0	195.0	6.31 L
65R20MFS10	0.30	650.0	520.0	130.0	842.0	661.0	73.0	195.0	6.31 L
65R20MFS30	0.30	650.0	520.0	130.0	842.0	515.0	219.0	195.0	6.31 L
65R0MFS0	0.40	650.0	650.0	0	749.0	653.0	0	260.0	6.31 L
65R20MFS0	0.40	650.0	520.0	130.0	749.0	653.0	0	260.0	6.31 L
65R20MFS10	0.40	650.0	520.0	130.0	749.0	588.0	65.0	260.0	6.31 L
65R20MFS30	0.40	650.0	520.0	130.0	749.0	455.0	195.0	260.0	6.31 L

Note: **Remark:** [1] **XRYUZ** denotes the following: **X** is the powder material content (OPC + RHA) (550 kg/m^3) and 650 kg/m^3); **RY** is the percentage OPC replacement of RHA content (0 and 20 wt.%); and **MFSZ** is the percentage rock replacement of MFS content (0, 10, and 30 wt.%).

4.1 Fresh-State Properties of SCC

In this case, the mix design concentrated on two main properties of the SCC mixtures in their current state, namely, the diameters of the slump flow and the J-ring and the amount of time needed for each specimen to pass through the V-funnel. A summary of the results relating to the fresh state of the SCC specimens and the SCC control is provided in Tab. 3. The results show that the diameter of the slump flow was between 65.1 ± 0.34 cm and 68.8 ± 0.52 cm for a w/p ratio of 0.40. The diameter of the slump flow was within 65.0 cm to 85.0 cm in accordance with EFNARC [25] guidelines. The w/p represented

the amount of water needed during the fabrication of the SCC specimens to aid in attaining the required slump level [28].

When concrete flows within a narrow space, the mortar's flow of rotation and the proportion of coarse aggregates influence the concrete's ability to overcome obstructing material [20]. Thus, based on the difference between the diameter of the slump flow and the J-ring, the SCC mixture's ability to penetrate tight openings was determined. The results indicated that the difference varied from 1.1 ± 0.01 cm to 7.2 ± 0.11 cm. While the time needed for the RHA-SCC to pass through the V-funnel was longer as compared to conventional SCC, the difference between the diameter of the slump flow and the J-ring indicated the level of blocking. For example, a difference of between 0 cm and 0–2.5 cm was considered to have "no visible blocking." This was observed when the SCC specimens at 550 kg/m^3 and 650 kg/m^3 were evaluated with a w/p of 0.40. A difference of between 2.5 cm and 5.0 cm was considered as having "minimal to noticeable blocking." Lastly, a difference of greater than 5.0 cm was considered to have "extreme blocking." It was observed that the content of the SCC specimens exhibited extreme blocking only when the w/p was 0.30. Extreme blocking was mainly characterized by a low binding capacity at 550 kg/m^3 and low water content, both of which reduced flowability. However, an increase in the binding content caused an increase in the flowability of the SCC mixture. This was attributed to the increase in the volume of pastes associated with the fine aggregates. Additionally, the MFS and RHA absorbed significantly more water than the coarse aggregate did. On the other hand, the control SCC did not provide any visible blocking given that the difference between the diameter of the slump flow and the J-ring ranged from 1.0 cm to 2.0 cm. All these findings are consistent with the findings reported in the existing literature [20,29].

Table 3: Fresh state properties of SCC mixes

Mixture label	w/p ratio	Slump flow (cm)	J-ring test (cm)	Difference (initial)	Blocking assessment	V-funnel flow time (initial) (s)	Unit weight	
							kg/m^3	% control
55R0MFS0	0.30	65.1 ± 0.34	64.0 ± 0.51	1.1 ± 0.03	No visible blocking	7.4 ± 0.04	2,389 ± 12.04	100.00
55R20MFS0	0.30	65.6 ± 0.15	63.3 ± 0.19	2.3 ± 0.07	Noticeable blocking	9.1 ± 0.02	2,369 ± 17.31	−0.84
55R20MFS10	0.30	66.2 ± 0.06	62.5 ± 0.11	3.7 ± 0.10	Noticeable blocking	18.1 ± 0.04	2,481 ± 22.89	3.85
55R20MFS30	0.30	67.8 ± 0.14	60.6 ± 0.48	7.2 ± 0.11	Extreme blocking	22.3 ± 0.08	2,589 ± 24.15	8.37
55R0MFS0	0.40	66.7 ± 0.63	65.1 ± 0.31	1.6 ± 0.02	No visible blocking	5.3 ± 0.01	2,371 ± 10.33	100.00
55R20MFS0	0.40	66.1 ± 0.55	64.9 ± 0.24	1.2 ± 0.01	Noticeable blocking	8.4 ± 0.02	2,356 ± 11.78	−0.63
55R20MFS10	0.40	67.4 ± 0.11	63.6 ± 0.20	3.8 ± 0.06	Noticeable blocking	14.2 ± 0.08	2,454 ± 14.81	3.50
55R20MFS30	0.40	67.8 ± 0.21	63.7 ± 0.56	4.1 ± 0.09	Noticeable blocking	17.7 ± 0.01	2,551 ± 15.98	7.59
65R0MFS0	0.30	67.4 ± 0.39	66.3 ± 0.42	1.1 ± 0.01	No visible blocking	5.2 ± 0.02	2,439 ± 20.01	100

(Continued)

Table 3 (continued).

Mixture label	w/p ratio	Slump flow (cm)	J-ring test (cm)	Difference (initial)	Blocking assessment	V-funnel flow time (initial) (s)	Unit weight	
							kg/m^3	% control
65R20MFS0	0.30	67.7 ± 0.08	66.7 ± 0.09	1.0 ± 0.05	No visible blocking	7.1 ± 0.04	2,431 ± 21.47	−0.33
65R20MFS10	0.30	67.9 ± 0.40	65.8 ± 0.24	2.1 ± 0.06	Noticeable blocking	13.2 ± 0.02	2,531 ± 18.64	3.77
65R20MFS30	0.30	67.9 ± 0.45	64.7 ± 0.31	3.2 ± 0.04	Noticeable blocking	18.3 ± 0.01	2,581 ± 19.52	5.82
65R0MFS0	0.40	68.8 ± 0.52	67.6 ± 0.21	1.2 ± 0.09	No visible blocking	3.4 ± 0.06	2,387 ± 14.81	100
65R20MFS0	0.40	67.7 ± 0.29	66.9 ± 0.29	0.8 ± 0.04	No visible blocking	6.2 ± 0.05	2,381 ± 13.95	−0.25
65R20MFS10	0.40	67.5 ± 0.16	65.8 ± 0.13	1.7 ± 0.06	Noticeable blocking	19.3 ± 0.02	2,464 ± 9.94	3.23
65R20MFS30	0.40	67.2 ± 0.23	64.6 ± 0.20	2.6 ± 0.07	Noticeable blocking	14.4 ± 0.02	2,507 ± 19.11	5.03

Note: **Remark:** [1] For the blocking assessment, the differences in the slump flow and J-ring flow diameters were determined. In this assessment, 0–2.5 cm is defined as no visible blocking; 2.5–5.0 cm is defined as minimal to noticeable blocking; and >5.0 cm is defined as noticeable to extreme blocking.

Further, in the present study, the V-funnel test was used to evaluate the viscosity of the concrete. According to EFNARC [25] guidelines, the time needed for the V-funnel should range from 6 s to 12 s. However, the time spent in the V-funnel varied considerably. For the SCC mixture of 550 kg/m^3 with a w/p of 0.30, the range was 7.4 ± 0.04 to 22.3 ± 0.08 s, with the maximum outcome obtained by 55R20MFS30; for the SCC mixtures of 650 kg/m^3 with a w/p of 0.40, the range was 3.4 ± 0.06 s to 14.4 ± 0.02 s. It is evident, therefore, that only three elements influenced the amount of time spent in the V-funnel: the SCC mixture, the w/p, and the MFS content. However, existing studies have associated the reduction in duration to the quantity of MFS used, which is, in turn, related to reduced workability [12].

In terms of workability, in the present study, the question is examined as to whether an increase in the proportion of RHA in SCC could improve the latter's fresh-state properties. This question arose from the idea that workability was minimized as a result of fine aggregates being more absorptive as compared to cement [16,30]. The results showed that unit weight ranged from 2371 ± 10.33 kg/m^3 to 2589 ± 24.15 kg/m^3, representing an increase of approximately 7.74% compared to control SCC. Thus, as a result of the high density associated with MFS, the specimens developed using both RHA and MFS were heavier than the control SCC, which did not include MFS in its composition. This result suggests that when used in the production of concrete, MFS tends to present better properties than the natural aggregates do. However, in comparison with the control SCC, the SCC mixture that included RHA in its composition was lighter, a result that was attributed to the latter mixture's inclusion of reactive amorphous silica, which is associated with low density [31].

4.2 Hardened-State Properties of SCC

The hardened properties of the SCC specimens and the control are subdivided into three main areas, which address distinct strength properties at 360 days: compressive strength, splitting tensile strength, and modulus of elasticity (MOE).

4.2.1 Compressive Strength

The compressive strength of the SCC mixture and the control SCC at 550 kg/m^3 and 650 kg/m^3 were compared in order to determine the relationship between this kind of strength and the bonding structure of the concrete. The three concrete samples were observed continuously for 360 curing days (Figs. 3 and 4). The data showed that the compressive strength of SCC mixtures was much higher than that of the control SCC created from cement and natural aggregates. For instance, the SCC specimen with a content of 550 kg/m^3 and a w/p of 0.30 exhibited compressive strength at 360 days of between 64.91 ± 3.35 N/mm^2 to 81.68 ± 4.57 N/mm^2, whereas the SCC specimen with the same content and a w/p of 0.40 exhibited compressive strength of between 57.50 ± 2.97 N/mm^2 and 73.35 ± 4.02 N/mm^2. On the other hand, the SCC specimen with a content of 650 kg/m^3 with a w/p of 0.30 exhibited compressive strength of between 78.96 ± 5.74 N/mm^2 and 93.93 ± 7.25 N/mm^2, whereas the SCC mixture with the same content but with a w/p of 0.40 exhibited compressive strength of between 65.81 ± 3.79 N/mm^2 and 84.43 ± 6.61 N/mm^2.

Additionally, the proportions of RHA and MFS affected the compressive strength of the concrete. The results indicated that an increase in the proportion of RHA such that the proportion of MFS decreased in the SCC specimens yielded greater compressive strength. This effect was noted for SCC specimens with 550 kg/m^3 as compared to those with 650 kg/m^3. Further, compared with the SCC specimen with a w/p of 0.40, the SCC specimen with a w/p of 0.30 exhibited greater compressive strength.

These results are consistent with the results reported in the existing literature that compare the compressive strengths of SCC samples and control SCC. For example, Jiang et al. discovered a strong bond between MFS and the paste [1]. Rehman et al. further indicated that the compressive strength of SCC decreased significantly when MFS was used as an approximately 30 wt.% replacement for natural aggregates [10].

4.2.2 Splitting Tensile Strength

The SCC specimens and the control SCC were evaluated in relation to tensile strength to understand how this hardened property of concrete was affected by the design of each of these [29]. The difference between the tensile strength and the compressive strength of the SCC mixtures of 550 kg/m^3 and 650 kg/m^3 was also determined. This difference is attributable to two main reasons: the use of an interfacial transition zone between the OPC and the MFS and the angular form of the MFS particles, which are solely responsible for the structure of the concrete mixture [32].

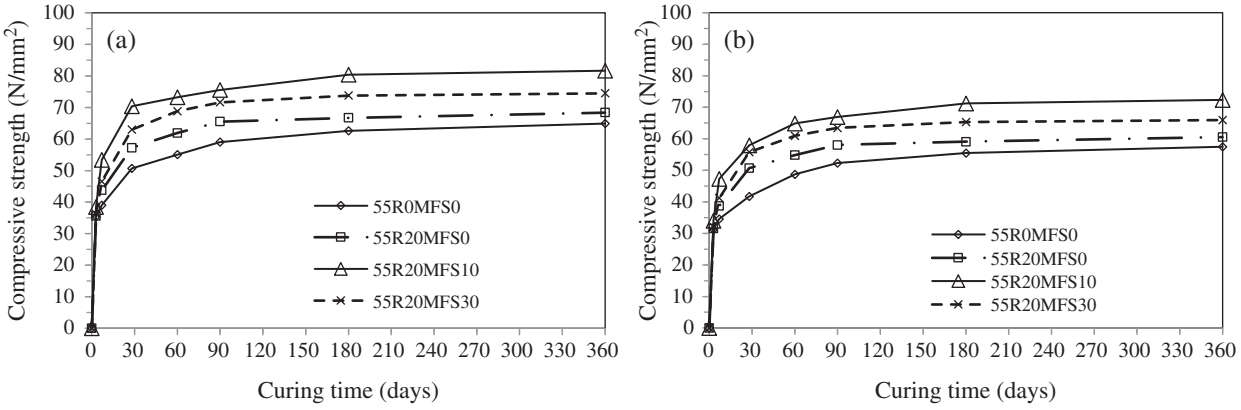

Figure 3: Compressive strength of SCC with (a) w/p = 0.30 and (b) w/p = 0.40 and a powder material content of 550 kg/m^3

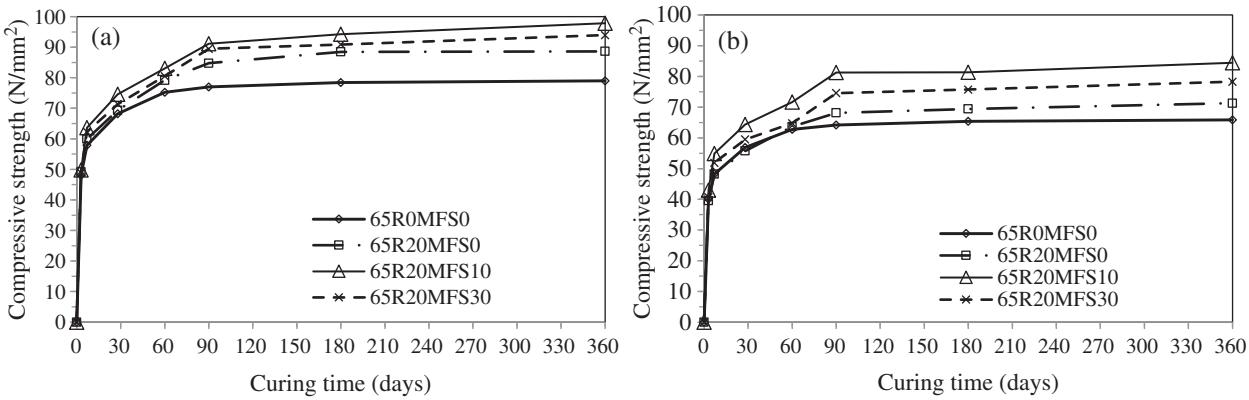

Figure 4: Compressive strength of SCC with (a) w/p = 0.30 and (b) w/p = 0.40 and a powder material content of 650 kg/m^3

The results, which indicate several outcomes, are presented in Figs. 5 and 6. First, the results show that the splitting tensile strength of the SCC mixtures increased exponentially as the curing period increased. Second, a similar trend to that for compressive strength was observed in relation to the splitting tensile strength of RHA and MFS. Third, a decrease in the ratio between splitting tensile strength and compressive strength was observed with an increasing proportion of MFS. This trend, however, was contrary to that shown by the control SCC. These results concur with the findings of existing studies in which 20 wt.% of RHA was used to increase the tensile strength of the control SCC based on the microstructure of the SCC mixture [13,30]. In line with the existing studies, this result suggests that an increase in the proportion of RHA in SCC is likely—as a result of RHA's micro-filling effects—to have a positive influence on the hardened properties of concrete [9].

4.2.3 Modulus of Elasticity

In relation to construction materials, the MOE refers to a property that can extend the durability, density, and thus, the safety of most concrete structures [17]. In the present study, the MOE of the SCC mixture and the control SCC using 550 kg/m^3 and 650 kg/m^3 was examined in order to understand its effect on the concrete's structure. The MOE of SCC specimens was observed after 28 curing days. The results indicated that the SCC specimens of 550 kg/m^3 with a w/p of 0.30 or 0.40 had MOE values of 44.4 GPa (44.4 × 10^3 N/mm^2) and 38.6 GPa (38.6 × 10^3 N/mm^2), respectively. These results were obtained after RHA was used as a 20 wt.% replacement for cement. A trend graph representing the MOE of the SCC mixtures is presented in Fig. 7.

Further, when MFS was used to substitute 10 wt.% of the coarse aggregates, the elasticity of the SCC specimens at 28 curing days was enhanced by 49.6 GPa (49.6 × 10^3 N/mm^2) and 45.7 GPa (45.7 × 10^3 N/mm^2) for the w/p ratios of 0.30 and 0.40, respectively. When RHA was used as a 20 wt.% replacement for cement, the SCC specimens of 650 kg/m^3 with a w/p ratio of 0.30 or 0.40 were shown to have elasticities of 50.2 GPa (49.6 × 10^3 N/mm^2) and 42.7 GPa (42.7 × 10^3 N/mm^2), respectively. Additionally, when MFS was used as a 10 wt.% replacement for coarse aggregates, the MOEs of the SCC specimens with a w/p of 0.30 or 0.40 rose to 53.3 GPa (53.3 × 10^3 N/mm^2) and 48.9 GPa (48.9 × 10^3 N/mm^2), respectively. These results show that increasing the SCC content from 550 kg/m^3 to 650 kg/m^3 had the effect of increasing MOE, whereas increasing the w/p of the SCC from 0.30 to 0.40 tended to reduce the MOE. These findings are consistent with the existing literature related to the increase in the compressive strength of SCC [11,18,33,34]. In addition, the MOE increased when the MFS was utilized as a substitute for coarse aggregates [18,33]. However, the MOE of RHA and the MOE of MFS in the SCC specimens were found to be greater than in the control SCC [18].

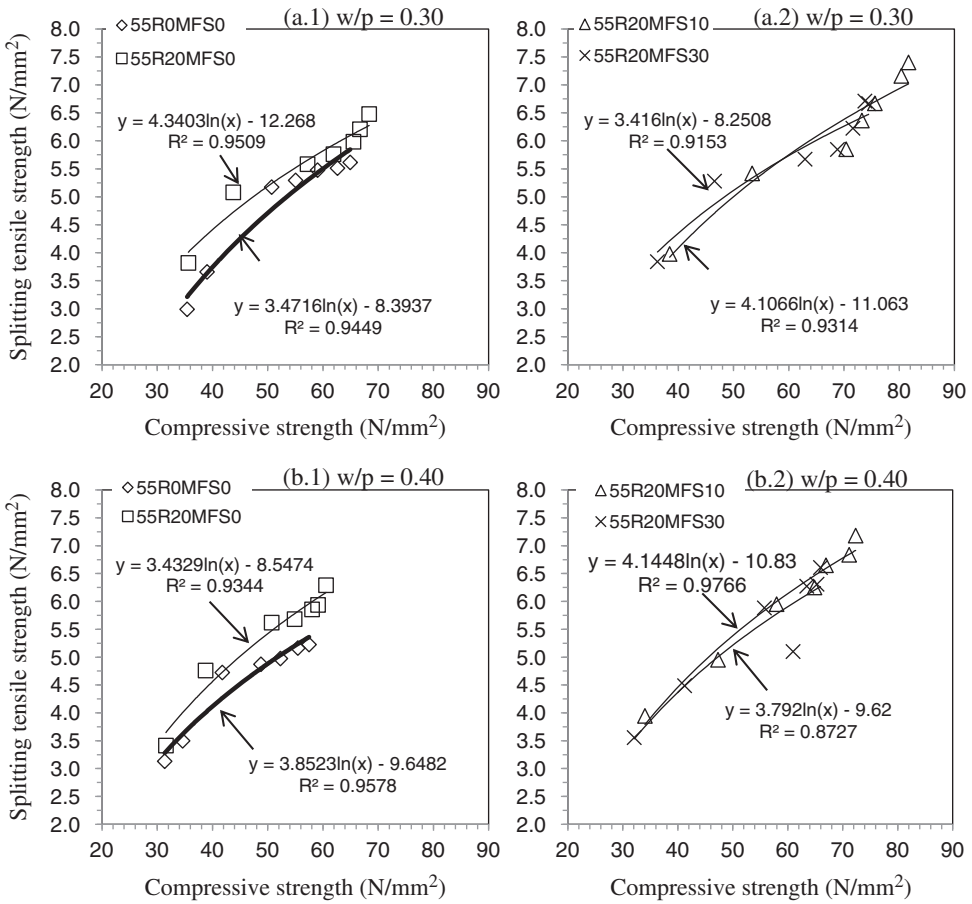

Figure 5: Relationship between the splitting tensile strength and compressive strength of SCC with (a) w/p = 0.30 and (b) w/p = 0.40 and a powder material content of 550 kg/m^3

4.3 Durability of SCC

In this section, results are presented pertaining to the durability properties of the SCC specimens obtained principally from the sulfate attack test and the acetic acid test.

4.3.1 Sulfate Attack

The results indicate a decrease in the expansion of the SCC with variations in the powder material content of 550 kg/m^3 (Fig. 8) and 650 kg/m^3 (Fig. 9). The SCC specimens with a powder material content of 550 kg/m^3 and a w/p of 0.30 were immersed in the Na_2SO_4 solution. In these conditions, the expansion at the long-term immersion point of 360 days as compared with that of the control SCC was as follows: For the SCC specimen that included in its composition 20 wt.% of MSF, expansion decreased by 3.07; for the specimen with 10 wt.% MSF, expansion decreased by 7.58%; for the specimen with 30 wt.% MSF, expansion decreased by 5.08%, for 0.30 w/p SCC, and 4.08% for 0.40-w/p SCC (Fig. 8). The decreased expansion of the SCC of 650 kg/m^3 is similar throughout 360 days (Fig. 9).

A further examination of the results indicated that the sulfate attack caused the pH of the water used in the production of the concrete to drop, thereby reducing the strength of the resulting specimens [32]. This is in contrast to the use of RHA, which, in alkaline conditions, increases the strength of the concrete in which it is used.

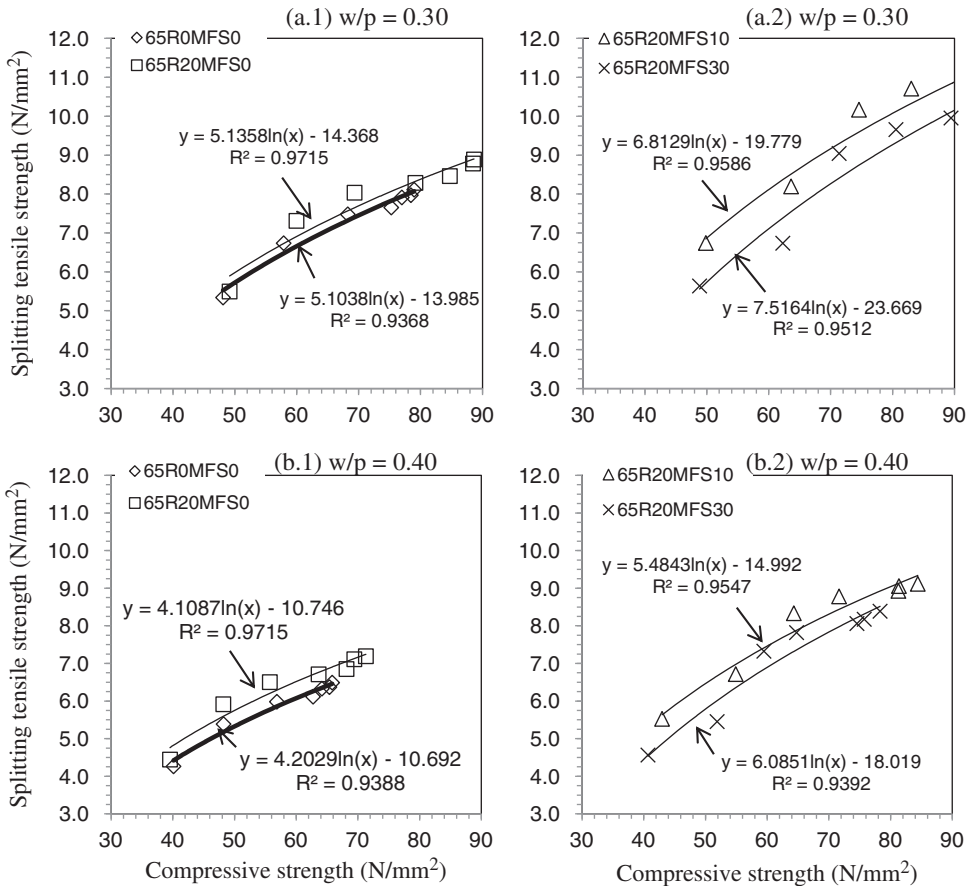

Figure 6: Relationship between the splitting tensile strength and compressive strength of SCC with (a) w/p = 0.30 and (b) w/p = 0.40 and a powder material content of 650 kg/m^3

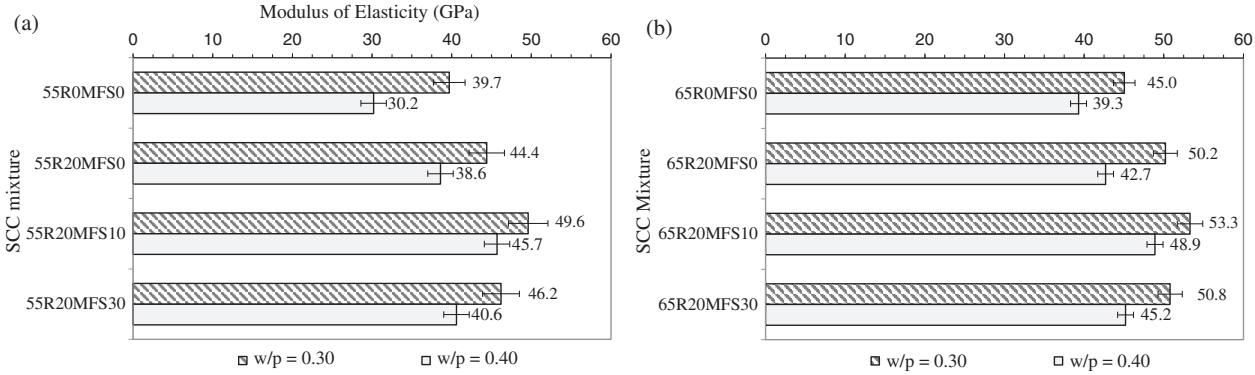

Figure 7: Modulus of elasticity of SCC with a powder material content of (a) 550 kg/m^3 and (b) 650 kg/m^3

Thus, it has been demonstrated that RHA is associated with increased expansion of concrete from immersion in a sulfate solution [35]. On this basis, it was anticipated that an SCC mixture into which RHA and MFS are incorporated would expand more than standard concrete made from cement and natural aggregates would. This suggests that SCC that has RHA and MFS included in its composition could be a good replacement for concrete with cement and natural aggregates that do not promote expansion [34].

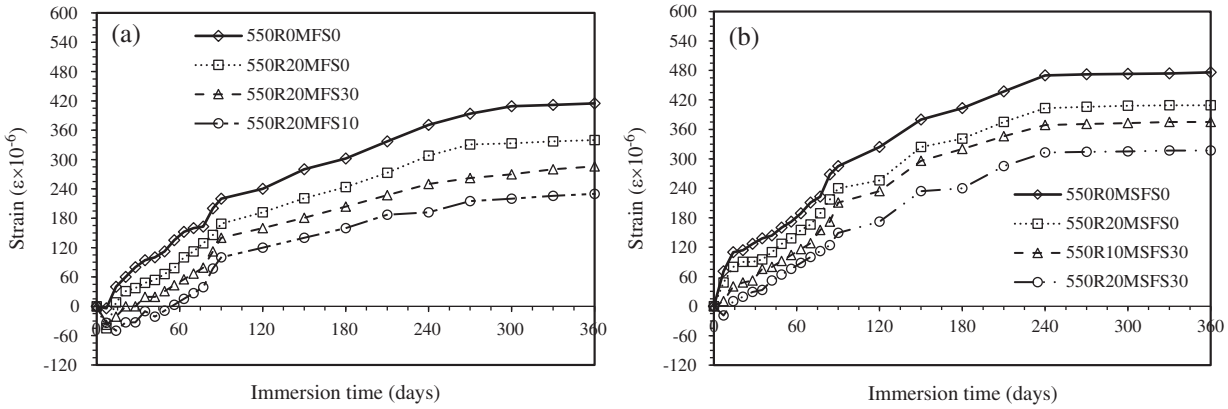

Figure 8: Expansion of SCC under immersion in an Na_2SO_4 solution with (a) w/p = 0.30 and (b) w/p = 0.40 and a powder material content of 550 kg/m^3

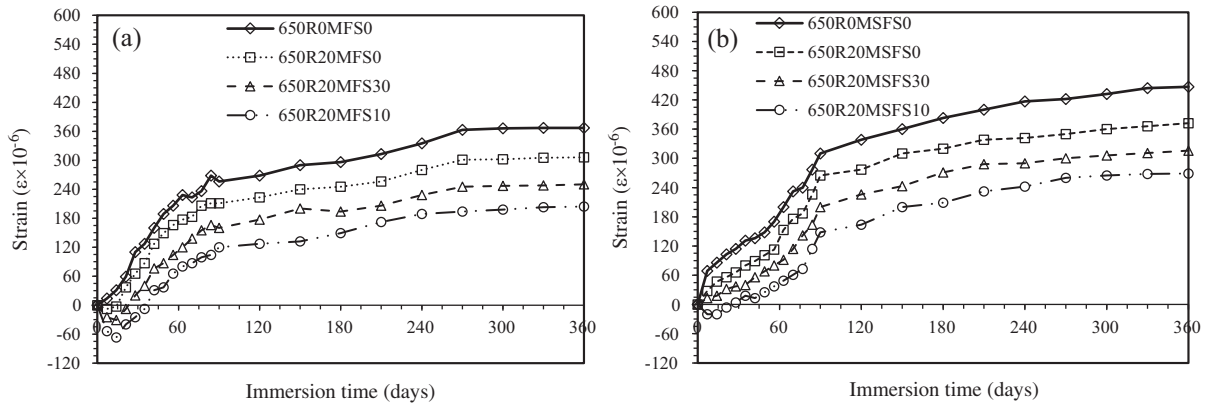

Figure 9: Expansion of SCC under immersion in an Na_2SO_4 solution with (a) w/p = 0.30 and (b) w/p = 0.40 and a powder material content of 650 kg/m^3

4.3.2 Acid Attack

Both the SCC specimens and the control SCC were immersed in CH_3COOH solutions of 3.0% concentration. To ensure optimum pH for the acetic solution, its pH was measured using a pH meter throughout the experiment. A pH value of 1.0 is considered optimum; therefore, 3.0% of the acetic acid was replaced with a new solution every month. Mass losses from the specimen with progressive immersion were observed. Summaries of the mass loss that occurred in the SCC specimens when exposed to CH_3COOH at intervals of 7 and 360 days are given in Figs. 10 and 11. The results indicated a decreased mass loss in the SCC specimens when exposed to the CH_3COOH solution for 360 immersion days. For the SCC specimen of 550 kg/m^3 with a w/p of 0.30, a decrease of mass loss accrued, ranging from 3.8 to 26.2%. Further, when the w/p proportion was 0.40, a mass loss accrued ranging from 4.5 to 12.4%. These results were recorded after the SCC mixture had been examined at 28 days to 90 days of curing following exposure to the CH_3COOH solution. For the SCC specimen of 650 kg/m^3 with a w/p of 0.30, decreased mass loss accrued of between 2.1 and 9.1%. However, for specimens with a w/p of 0.40, the mass loss was between 2.6 and 7.6%. Throughout the entire study, pozzolan was employed to reduce the loss of mass, which positively affected the durability of the SCC when exposed to the acidic solution. Based on these results, RHA used as a replacement for cement could provide effective resistance to the mass loss that is attributed to the acidic solution [35,36]. Additionally, the capacity of the SCC mixture to

resist mass loss was further reduced when MFS was used in place of natural aggregates. Therefore, a combination of RHA and MFS in SCC could provide better resistance to mass loss than is the case for standard SCC mixtures as a result of the durability properties [37,38].

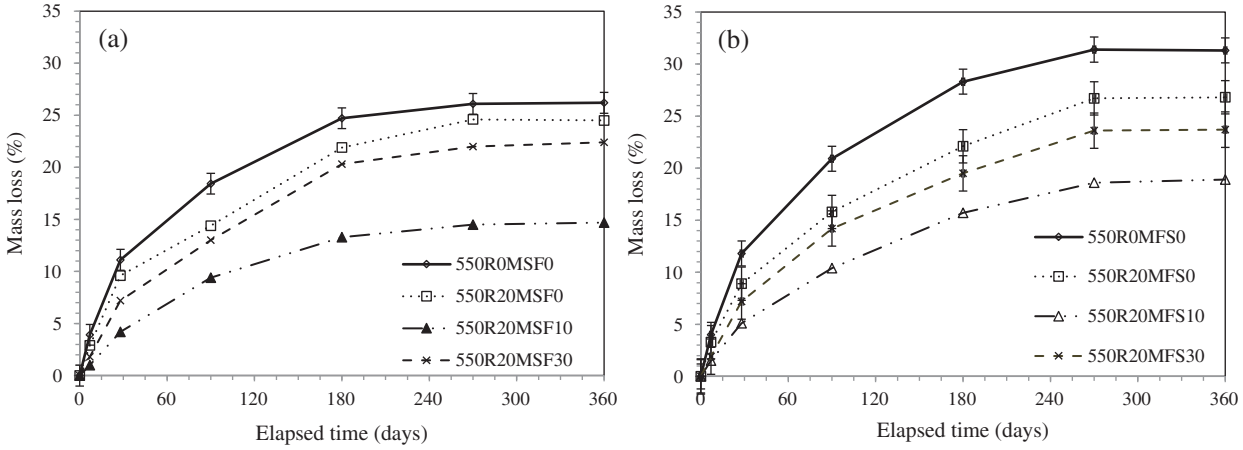

Figure 10: Mass loss of SCC under immersion in CH_3COOH with (a) w/p = 0.30 and (b) w/p = 0.40 and a powder material content of 550 kg/m^3

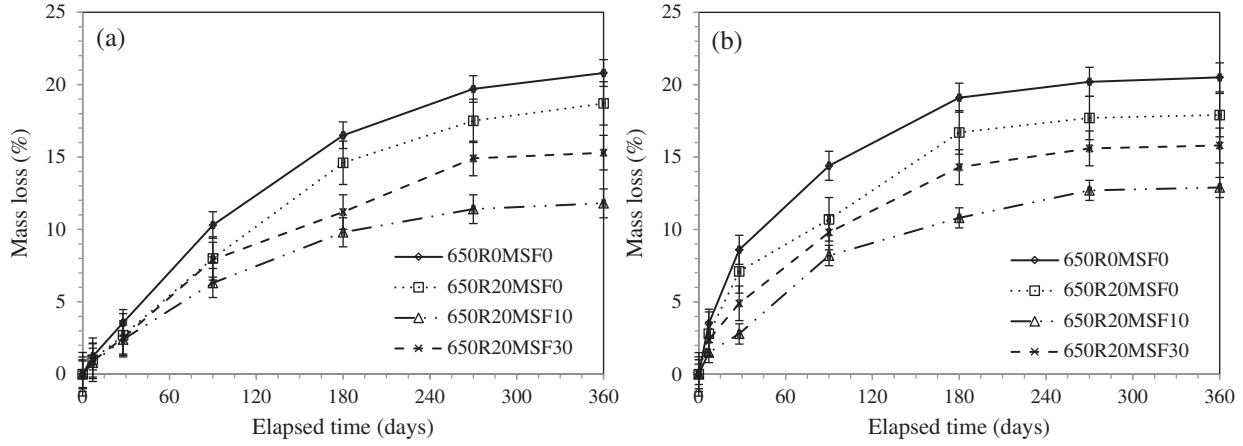

Figure 11: Mass loss of SCC under immersion in CH_3COOH with (a) w/p = 0.30 and (b) w/p = 0.40 and a powder material content of 650 kg/m^3

5 Implications for Material Construction

Exposing concrete to harsh environmental conditions has led to uncontrolled problems in wastewaters and sewage plants. Based on this study's results, there is a need for extreme caution in taking steps to improve the durability, hardened-state, and fresh-state properties of the concrete [36]. It was further noted that exposure to acid and sulfate had a negative impact on the structure of the concrete, which eventually led to a decrease in its mechanical strength. For concrete to withstand exposure to chemicals such as acetic acid and sodium sulfate, the study results show that RHA, in conjunction with pozzolanic material, could be used to replace cement in the concrete mixture [39]. Overall, given its tendency to the adverse effects of acids and sulfates, RHA could be an effective alternative to cement [34,39].

The mechanical strength of the SCC mixture was also evaluated, with the results indicating that 20 wt.% of RHA and 10 wt.% of MFS are required to optimize the mechanical properties of the SCC mixture. However, this result did not bond for SCC with cement content. For instance, the SCC specimen with a lower w/p and a higher cement content demonstrated an increase in strength, which is primarily attributable to the bond between the paste and the natural aggregates [18]. This result suggests that in the presence of a strong bond between the paste and the aggregates, a weaker coating layer tends to have an adverse effect on both the mechanical properties and the durability of SCC.

6 Conclusions

The purpose of this study was to examine the properties of SCC mixtures that included RHA and MFS in their composition as a possible replacement for the cement and natural coarse aggregate used in SCC. According to the experimental results, the following conclusions can be drawn:

In order to evaluate the fresh state of the SCC specimens, multiple tests were performed, including the V-funnel test and tests to determine workability and differences between the diameter of the slump flow and the J-ring. The results indicated that three factors—MFS and MFS content, powder content and w/p—influenced workability and the time it took for the specimens to pass through the V-funnel. Of all the mixtures, the control SCC passed through the V-funnel most quickly, thereby indicating that it had the highest level of workability. It was also noted that the SCC prepared with 20 wt.% and 30 wt.% MFS exhibited greater blocking ability as compared to the control SCC, which did not provide any visible blocking.

The hardened-state properties of the SCC specimens refer to compressive strength, tensile strength, and MOE. Measured at 360 curing days, the compressive strength of the SCC was significantly higher than that of the control SCC. The RHA and MFS positively influenced the compressive and splitting tensile strengths at long-term state. The results indicated that the tensile strength of the SCC increased exponentially over time whereas the tensile strength of the control, which was very low, remained steady over the same period. In regard to elasticity, an increase in the SCC content from 550 kg/m^3 to 650 kg/m^3 had a positive impact on elasticity. On the other hand, an increase in the w/p from 0.30 to 0.40 had a negative influence on elasticity.

In order to explore the durability performance of the SCC specimens and the control, all were subjected to sulfate and acetic attack tests. From the sulfate attack, the SCC specimens were shown to expand to a greater extent than did the control SCC with different w/p—a result attributable to the formation of ettringite crystals in the SCC specimens, which had the effect of increasing the mass or each of these.

Based on the findings regarding the fresh-state, hardened-state, and durability properties, it can be concluded that including RHA and MFS in SCC has the effect of significantly improving the structure of the concrete. Thus, RHA and MFS should be considered suitable replacements for cement and natural aggregates in the production of concrete at a proportion of 10% MFS and 20% RHA to achieve the greatest strength development and the highest level of durability.

Funding Statement: This research was funded by Faculty of Engineering, King Mongkut's University of Technology North Bangkok, Contact No. ENG-62-48. This research has also received funding from the European Union's Horizon 2020 Research and Innovation Programme under Grant Agreement No. 777823.

Conflicts of Interest: The authors declare that they have no conflicts of interest to report regarding the present study.

References

1. Jiang, Y., Ling, T. C., Shi, C., Pan, S. Y. (2018). Characteristics of steel slags and their use in cement and concrete: a review. *Resources, Conservation and Recycling, 136(76),* 187–197. DOI 10.1016/j.resconrec.2018.04.023.
2. Tamayo, P., Pacheco, J., Thomas, C., de Brito, J., Rico, J. (2020). Mechanical and durability properties of concrete with coarse recycled aggregate produced with electric arc furnace slag concrete. *Applied Sciences, 10(1),* 216. DOI 10.3390/app10010216.

3. Anastasiou, E., Filikas, K. G., Stefanidou, M. (2014). Utilization of fine recycled aggregates in concrete with fly ash and steel slag. *Construction and Building Materials, 50(10),* 154–161. DOI 10.1016/j.conbuildmat.2013.09.037.
4. Vijayaraghavan, J., Jude, A. B., Thivya, J. (2017). Effect of copper slag, iron slag and recycled concrete aggregate on the mechanical properties of concrete. *Resources Policy, 53(5),* 219–225. DOI 10.1016/j.resourpol.2017.06.012.
5. Palankar, N., Shankar, A. R., Mithun, B. M. (2016). Durability studies on eco-friendly concrete mixes incorporating steel slag as coarse aggregates. *Journal of Cleaner Production, 129(3),* 437–448. DOI 10.1016/j.jclepro.2016.04.033.
6. Brand, A. S., Roesler, J. R. (2015). Steel furnace slag aggregate expansion and hardened concrete properties. *Cement and Concrete Composites, 60(3),* 1–9. DOI 10.1016/j.cemconcomp.2015.04.006.
7. Renz, A., Solas, M. Z., Almeida, P. R., Buhler, M., Gerbert, P. et al. (2016). Shaping the future of construction: A breakthrough in mindset and technology. *World Economic Forum, 7,* 1–64.
8. Sua-Iam, G., Makul, N. (2015). Utilization of coal-and biomass-fired ash in the production of self-consolidating concrete: a literature review. *Journal of Cleaner Production, 100(5),* 59–76. DOI 10.1016/j.jclepro.2015.03.038.
9. Ziari, H., Hayati, P., Sobhani, J. (2017). Air-entrained air field self-consolidating concrete pavements: strength and durability. *International Journal of Civil Engineering, 15(1),* 21–33. DOI 10.1007/s40999-016-0104-4.
10. Rehman, S., Iqbal, S., Ali, A. (2018). Combined influence of glass powder and granular steel slag on fresh and mechanical properties of self-consolidating concrete. *Construction and Building Materials, 178(97),* 153–160. DOI 10.1016/j.conbuildmat.2018.05.148.
11. Hisham, Q. (2020). Hardened properties of green self-consolidating concrete made with steel slag coarse aggregates under hot conditions. *ACI Materials Journal, 117(1),* 107–118.
12. Qasrawi, H. (2018). Fresh properties of green SCC made with recycled steel slag coarse aggregate under normal and hot weather. *Journal of Cleaner Production, 204(9),* 980–991. DOI 10.1016/j.jclepro.2018.09.075.
13. Kannan, V. (2018). Strength and durability performance of self-consolidating concrete containing self-combusted rice husk ash and metakaolin. *Construction and Building Materials, 160,* 169–179. DOI 10.1016/j.conbuildmat.2017.11.043.
14. Hakas, P., Martyana, D. C., Monika, F. (2020). Fresh properties characteristics and compressive strength of fiber self-compacting concrete incorporated with rice husk ash and wire steel fiber. *International Journal of Sustainable Construction Engineering and Technology, 11(1),* 290–299.
15. Abdul Rahim, M., Ibrahim, N. M., Idris, Z., Ghazaly, Z. M., Shahidan, S. et al. (2014). Properties of concrete with different percentange of the rice husk ash (RHA) as partial cement replacement. *Materials Science Forum, 803,* 288–293. DOI 10.4028/www.scientific.net/MSF.803.288.
16. Sua-iam, G., Makul, N., Cheng, S., Sokrai, P. (2019). Workability and compressive strength development of self-consolidating concrete incorporating rice husk ash and foundry sand waste: a preliminary experimental study. *Construction and Building Materials, 228,* 116813. DOI 10.1016/j.conbuildmat.2019.116813.
17. Patel, Y. J., Shah, N. (2018). Enhancement of the properties of ground granulated blast furnace slag based self-consolidating geopolymer concrete by incorporating rice husk ash. *Construction and Building Materials, 171(9),* 654–662. DOI 10.1016/j.conbuildmat.2018.03.166.
18. Dipendra, D., Ramesh, B., Nirmal, B., Keshav, B. (2020). Evaluation of rice husk ash as a partial replacement of cement in self-compacting concrete using mix design. *International Journal of Engineering Research & Technology, 9(7),* 1402–1409.
19. Le, H. T., Ludwig, H. M. (2016). Effect of rice husk ash and other mineral admixtures on properties of self-consolidating high performance concrete. *Materials & Design, 89,* 156–166. DOI 10.1016/j.matdes.2015.09.120.
20. Makul, N., Sua-iam, G. (2018). Effect of granular urea on the properties of self-consolidating concrete incorporating untreated rice husk ash: flowability, compressive strength and temperature rise. *Construction and Building Materials, 162(2016),* 489–502. DOI 10.1016/j.conbuildmat.2017.12.023.
21. Sobolev, K., Kozhukhova, M., Sideris, K., Menéndez, E., Santhanam, M. (2018). Alternative supplementary powder materials. *Properties of Fresh and Hardened Concrete Containing Supplementary Powder Materials,* 233–282.

22. Zareei, S. A., Ameri, F., Dorostkar, F., Ahmadi, M. (2017). Rice husk ash as a partial replacement of cement in high strength concrete containing micro silica: evaluating durability and mechanical properties. *Construction Materials, 7,* 73–81.
23. Deepankar, K. A., Surender, K. V. (2019). An overview on mixture design of self-compacting concrete. *Structural Concrete, 20(1),* 371–395. DOI 10.1002/suco.201700279.
24. Abdullah, M. Z., Ali, A. (2020). Influence of mixing time and superplasticizer dosage on self-consolidating concrete properties. *Journal of Materials Research and Technology, 9(3),* 6101–6115. DOI 10.1016/j.jmrt.2020.04.013.
25. The European Federation of Specialist Construction Chemicals and Concrete Systems (EFNARC) (2002). Specification and guidelines for self-consolidating concrete. Association House, Surrey, UK. *www.efnarc.org*
26. ASTM (2016). *Standard specification for portland cement,* vol. 4.01. Cement, Lime, Gypsum, Philadelphia: American Society for Testing and Materials.
27. ASTM (2016). *Standard specification for portland cement,* vol. 4.02. Philadelphia: Concrete and Aggregates, American Society for Testing and Materials.
28. Lim, J. S., Cheah, C. B., Ramli, M. B. (2019). The setting behavior, mechanical properties and drying shrinkage of ternary blended concrete containing granite quarry dust and processed steel slag aggregate. *Construction and Building Materials, 215,* 447–461. DOI 10.1016/j.conbuildmat.2019.04.162.
29. Sua-iam, G., Sokrai, P., Makul, N. (2016). Novel ternary blends of Type 1 Portland cement, residual rice husk ash, and limestone powder to improve the properties of self-consolidating concrete. *Construction and Building Materials, 125(1),* 1028–1034. DOI 10.1016/j.conbuildmat.2016.09.002.
30. Raisi, E. M., Amiri, J. V., Davoodi, M. R. (2018). Mechanical performance of self-consolidating concrete incorporating rice husk ash. *Construction and Building Materials, 177,* 148–157. DOI 10.1016/j.conbuildmat.2018.05.053.
31. Patel, Y. J., Shah, N. (2018). Enhancement of the properties of ground granulated blast furnace slag based self-consolidating geopolymer concrete by incorporating rice husk ash. *Construction and Building Materials, 171(9),* 654–662. DOI 10.1016/j.conbuildmat.2018.03.166.
32. Sharma, R., Khan, R. A. (2018). Influence of copper slag and metakaolin on the durability of self-consolidating concrete. *Journal of Cleaner Production, 171,* 1171–1186. DOI 10.1016/j.jclepro.2017.10.029.
33. Pan, Z., Zhou, J., Jiang, X., Xu, Y., Jin, R. et al. (2019). Investigating the effects of steel slag powder on the properties of self-consolidating concrete with recycled aggregates. *Construction and Building Materials, 200(4),* 570–577. DOI 10.1016/j.conbuildmat.2018.12.150.
34. Wang, G. C. (2016). *The utilization of slag in civil infrastructure construction*. Woodhead Publishing. Cambridge, UK. DOI 10.1016/B978-0-08-100381-7.00011-2.
35. Miller, S. A., Cunningham, P. R., Harvey, J. T. (2019). Rice-based ash in concrete: A review of past work and potential environmental sustainability. *Resources, Conservation and Recycling, 146(1),* 416–430. DOI 10.1016/j.resconrec.2019.03.041.
36. Rêgo, J. H. S., Nepomuceno, A. A., Figueiredo, E. P., Hasparyk, N. P. (2015). Microstructure of cement pastes with residual rice husk ash of low amorphous silica content. *Construction and Building Materials, 80(9),* 56–68. DOI 10.1016/j.conbuildmat.2014.12.059.
37. Long, G., Gao, Y., Xie, Y. (2015). Designing more sustainable and greener self-compacting concrete. *Construction and Building Materials, 84(3),* 301–306. DOI 10.1016/j.conbuildmat.2015.02.072.
38. Palankar, N., Shankar, A. R., Mithun, B. M. (2016). Durability studies on eco-friendly concrete mixes incorporating steel slag as coarse aggregates. *Journal of Cleaner Production, 129(3),* 437–448. DOI 10.1016/j.jclepro.2016.04.033.
39. Carro-López, D., González-Fonteboa, B., Brito, J. D., Martínez-Abella, F., González-Taboada, I. et al. (2015). Study of the rheology of self-compacting concrete with fine recycled concrete aggregates. *Construction and Building Materials, 96(6),* 491–501. DOI 10.1016/j.conbuildmat.2015.08.091.